

Synthesis of Copper Metallic Clusters Using Reverse Micelles as Microreactors

I. Lisiecki and M. P. Pileni*

Contribution from the Université P. et M. Curie, Laboratoire S.R.S.I., Bâtiment 74(F), 4 place Jussieu 75005 Paris, France, and C.E.N. Saclay, D.R.E.C.A.M.-S.C.M., Bâtiment 522, 91191 Gif sur Yvette, France

Received October 13, 1992

Abstract: Reverse micelles are used to synthesize in situ nanometallic copper particles. In mixed reverse micelles with hydrazine as a reducing agent, metallic copper particles are formed. At low water content, small particles are obtained. With increasing water content, the size of the metallic cluster increases from 2 to 10 nm. The use of pure copper surfactant molecules instead of mixed micelles favors the formation of cylindrical metallic particles. By using sodium borohydride as a reducing agent, in the absence of oxygen and at low water content, large metallic copper particles (from 20 to 28 nm) are formed. With increasing water content, the metallic clusters progressively disappear, forming instead copper oxide particles.

Introduction

Metals constitute a wide class of catalysts, and because catalysis occurs on the surface, there is a substantial economic incentive to obtain small monodisperse metallic particles. However, this raises two main problems. One is fundamental in nature and addresses the question discussed below, regarding the particle size at which metallic properties are lost. The other is more practical and concerns the preparation of very small particles.

Surfactants dissolved in organic solvents form spheroidal aggregates called reverse micelles.¹ Water is readily solubilized in the polar core, forming a so-called "water pool", characterized by w . With Aerosol OT (AOT) as surfactant, the maximum amount of bound water in the micelle corresponds to a water-surfactant molar ratio ($w = [\text{H}_2\text{O}]/[\text{AOT}]$) of about 6. Above $w = 15$, the water pool radius depends linearly on the water content ($r_w = 1.5 \times w$).² Another property of reverse micelles is their dynamic character.¹ Upon collision, reverse micelles exchange their water content, which makes possible coprecipitation or chemical reactions from reactants dissolved in separate droplets.

In this paper, we report the formation of metallic copper colloidal particles in reverse micelles. The size of the metallic particles increases with the water content. The shape of the clusters can be changed by using cylindrical reverse micelles. Metallic particles surrounded by an oxide monolayer or pure copper oxide also can be obtained.

Experimental Section

AOT and hydrazine were obtained from Sigma, isooctane from Fluka, and sodium borohydride, NaBH_4 , from Alfa. They were used without further purification. The synthesis of copper dioctyl sulfosuccinate, $\text{Cu}(\text{AOT})_2$, has been previously described.³

A reverse micellar solution is formed by solubilizing either pure copper AOT ($10^{-2} < [\text{Cu}(\text{AOT})_2] < 10^{-1}$ M) or a mixed micellar solution containing copper AOT and AOT surfactant, with the total concentration varying from 0.1 to 0.25 M. A reducing agent such as sodium borohydride, NaBH_4 , or hydrazine, N_2H_4 , is then added to the micellar solution.

Hydrazine is injected into a previously prepared reverse micellar solution. With NaBH_4 , two micellar solutions at fixed w are mixed. One

* Author to whom the correspondence should be addressed at the Université P. et M. Curie.

(1) *Structure and reactivity in reverse micelles*; Pileni, M. P., Ed.; Elsevier: Amsterdam, 1989.

(2) Pileni, M. P.; Zemb, T.; Petit, C. *Chem. Phys. Lett.* **1985**, *118*, 414.

(3) Pileni, M. P.; Motte, L.; Petit, C. *Chem. Mater.* **1992**, *4*, 338.

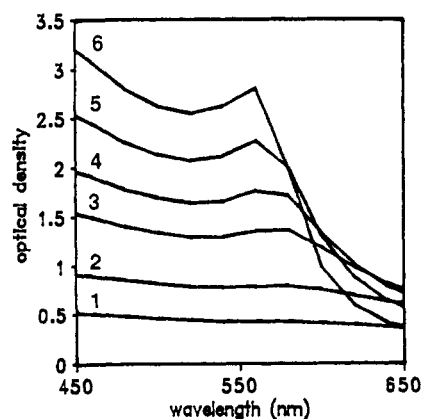


Figure 1. Simulated absorption spectra of metallic copper particles corresponding to various radii, r , of metallic particles: (1) $r = 0.5$, (2) $r = 1$, (3) $r = 2$, (4) $r = 3$, (5) $r = 5$, and (6) $r \geq 10$ nm.

contains the reducing agent and sodium AOT and the other mixed copper and sodium AOT.

Absorption spectra were recorded on Perkin-Elmer Lambda 5 and Hewlett-Packard HP 8452A spectrophotometers. A drop of this solution was evaporated under vacuum, and the electron micrograph was obtained with a Jeol electron microscope (Model Jem.100CX.2).

Results and Discussion

In aqueous solution the addition of a reducing agent such as hydrazine or sodium borohydride to an ionic copper solution induces precipitation of copper metal or bulk-phase oxide, whereas in reverse micellar solution, under various experimental conditions, particles clusters are formed. From these it can be concluded, as has been observed with CdS semiconductors,³ that AOT reverse micelles prevent precipitation.

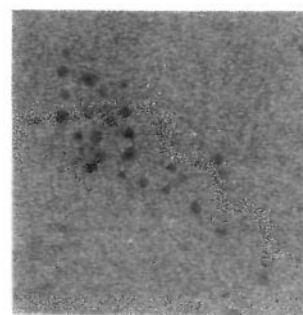
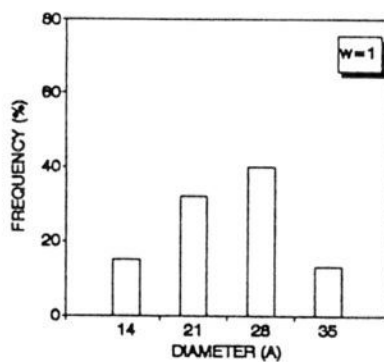
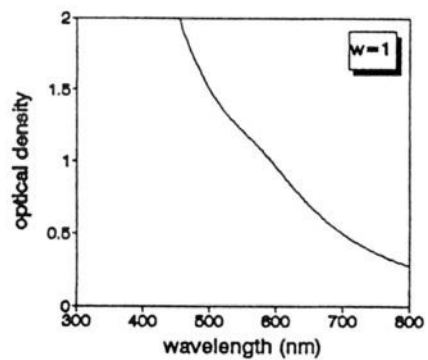
1. Change in the Absorption Spectrum with the Size of Metallic Clusters. Colloidal dispersions of metals exhibit absorption bands or broad regions of absorption in the ultraviolet-visible range. These are due to the excitation of plasma resonances or interband transitions and are a characteristic property of the metallic nature of the particles.

The absorption spectra of colloidal copper particles have been described, including the effect on the absorption spectra of varying

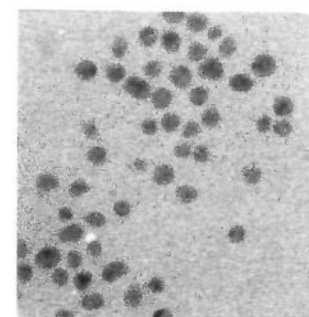
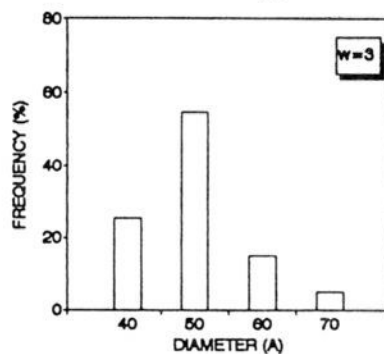
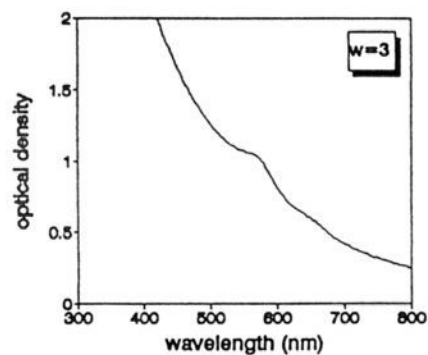
(4) Wokaun, A.; Gordon, J. P.; Liao, P. F. *Phys. Rev. Lett.* **1982**, *48*, 957.

(5) Meier, M.; Wokaun, A. *Optics Lett.* **1983**, *8*, 581.

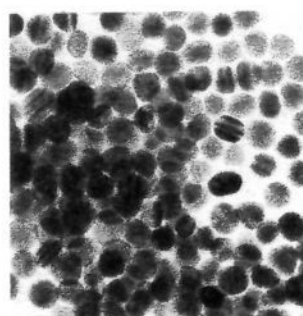
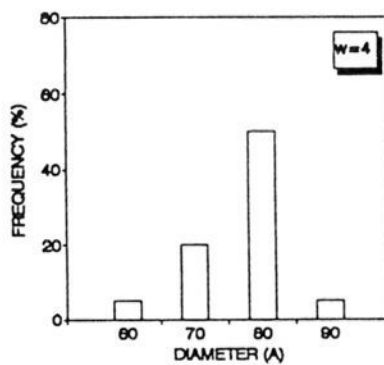
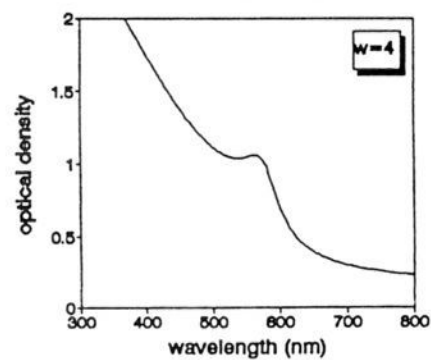
(6) Euler, J. Z. *Phys.* **1954**, *137*, 318.



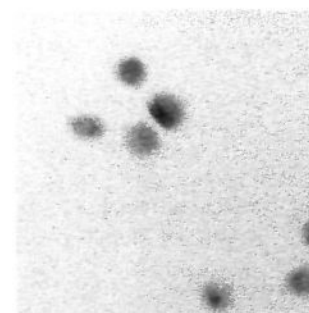
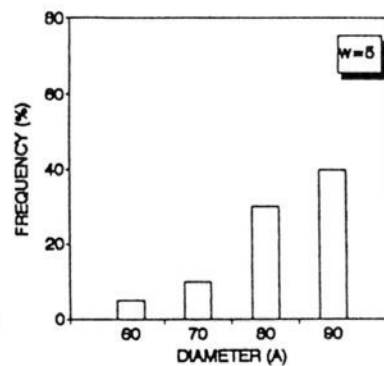
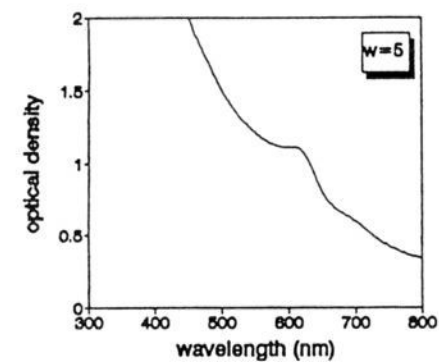
1mm=14Å



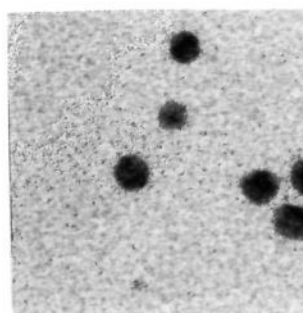
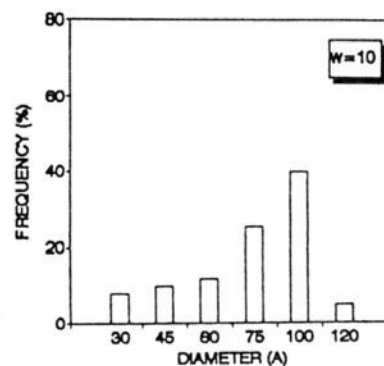
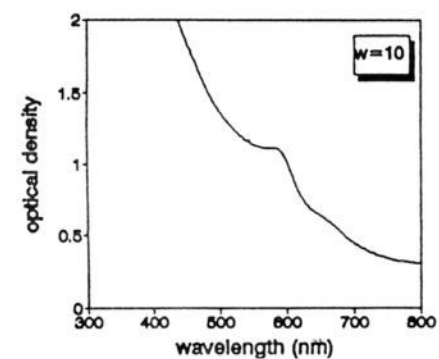
1mm=21Å



1mm=21Å



1mm=21Å



1mm=21Å

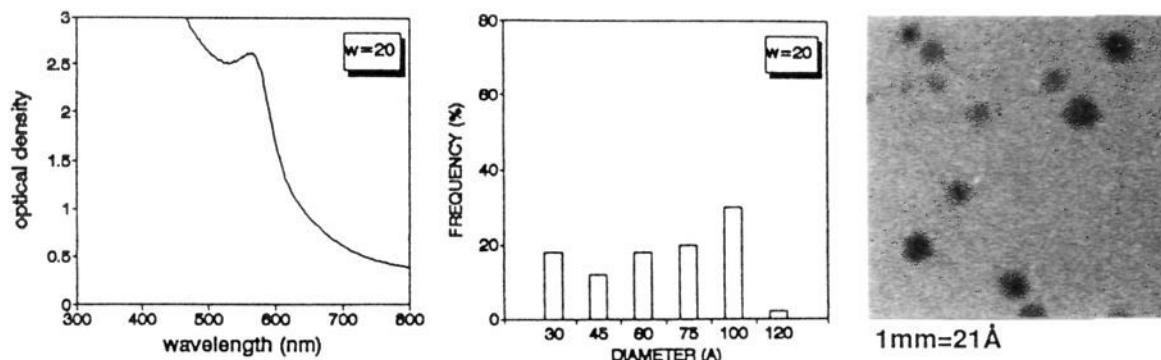


Figure 2. Absorption spectra, electron microscopy, and histograms of copper metallic particles prepared in reverse micelles with various water contents: $[\text{AOT}] = 0.1\text{ M}$; $[\text{Cu}(\text{AOT})_2] = 10^{-2}\text{ M}$; $[\text{N}_2\text{H}_4] = 2 \times 10^{-2}\text{ M}$. (Reproduced at 85% of original size.)

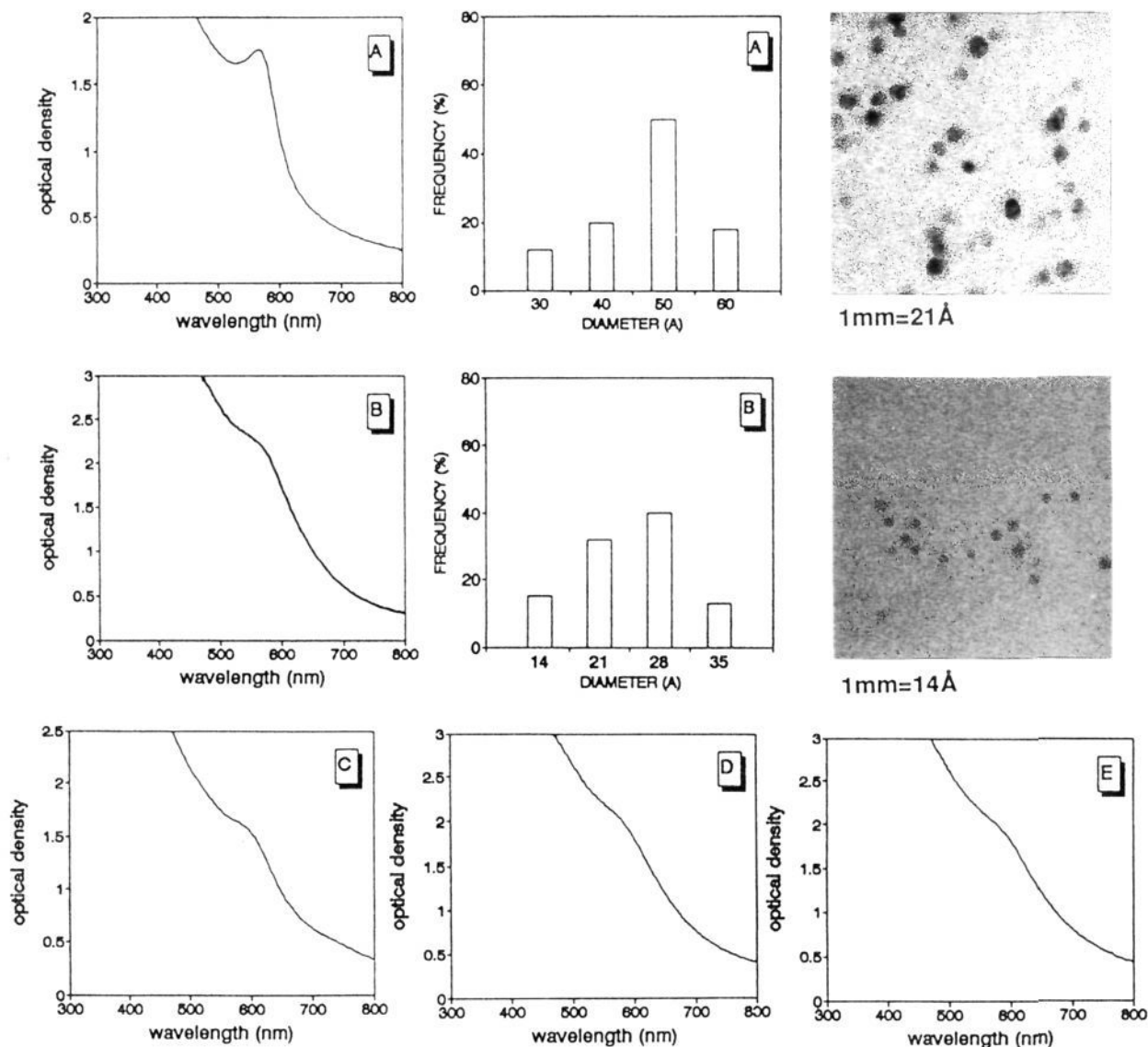


Figure 3. Absorption spectra, electron microscopy, and histograms of metallic copper particles formed in reverse micelles with variable AOT concentrations at $w = 1$: $[\text{Cu}(\text{AOT})_2] = 10^{-2}\text{ M}$, $[\text{N}_2\text{H}_4] = 2 \times 10^{-2}\text{ M}$. (A) $[\text{AOT}] = 5 \times 10^{-2}\text{ M}$. (B) $[\text{AOT}] = 10^{-1}\text{ M}$. (C) $[\text{AOT}] = 2 \times 10^{-1}\text{ M}$. (D) $[\text{AOT}] = 3 \times 10^{-1}\text{ M}$. (E) $[\text{AOT}] = 4 \times 10^{-1}\text{ M}$. (Reproduced at 85% of original size.)

the particle size. Indeed, if the particle dimensions⁴⁻⁶ are smaller than the mean free path of the conduction electrons, collisions of these electrons with the particle surface are noticed. This lowers the effective mean free path. By evaluating the absorption measurements of spherical copper particles (between 10 and 100

Å in diameter), Mies' theory⁷ can be used in the expanded versions discussed by different authors.⁸⁻¹¹ The absorbance A can be

(7) Mie, G. *Ann. Phys.* **1908**, 25, 377.

(8) Fragstein, C. V.; Roemer, H. Z. *Phys.* **1958**, 151, 54.

(9) Roemer, H.; Fragstein, C. V. Z. *Phys.* **1961**, 163, 27.

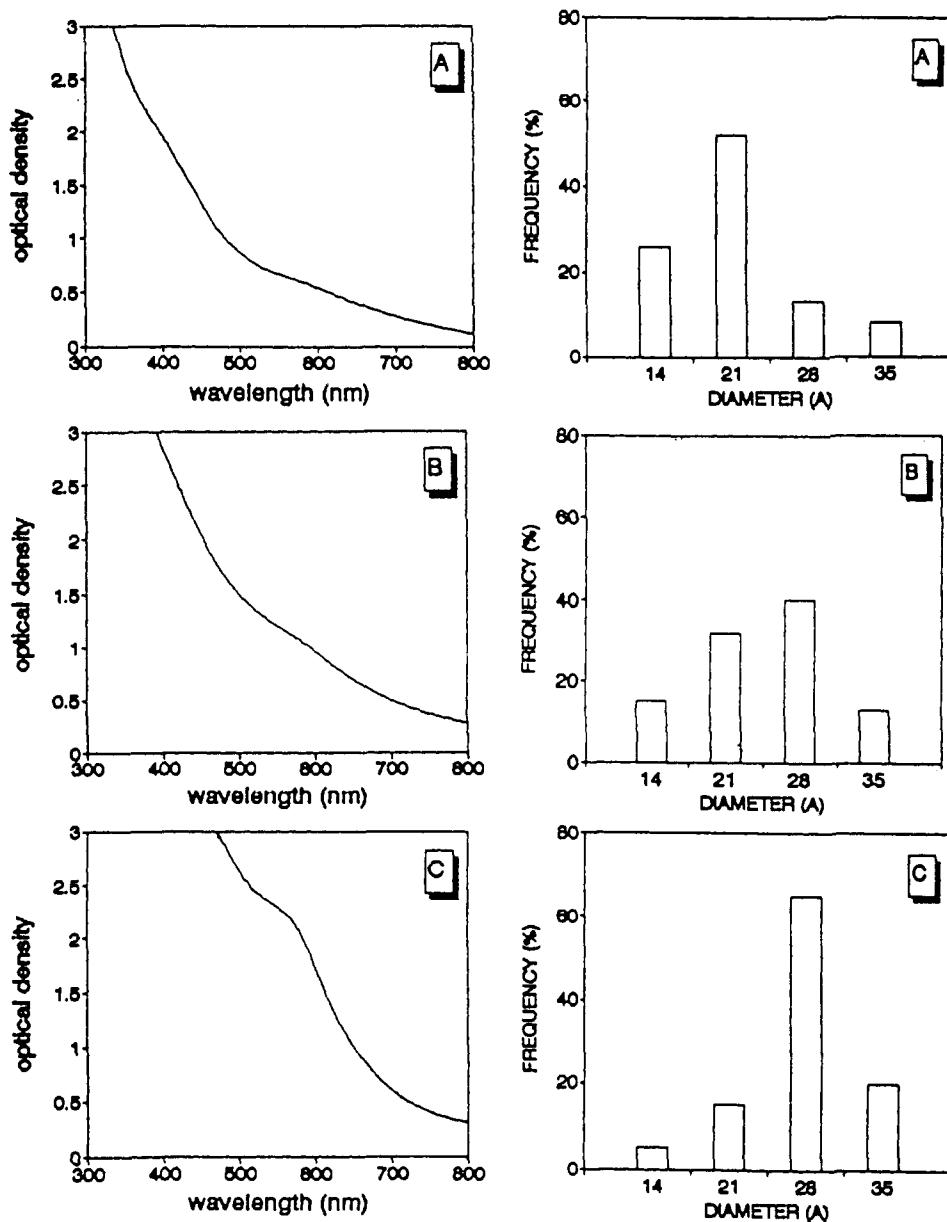


Figure 4. Variation of the absorption spectra and electron microscopy of the particles with time: $[AOT] = 0.1 \text{ M}$; $[\text{Cu}(AOT)_2] = 10^{-2} \text{ M}$; $[\text{N}_2\text{H}_4] = 2 \times 10^{-2} \text{ M}$. (A) 30 min. (B) 5 h. (C) 24 h, $w = 1$.

calculated for a dispersion of N particles per unit volume by the following equation:⁸⁻¹¹

$$A = \frac{CNl}{2.303}$$

where l and C are the optical pathlength and the cross section, respectively. In the limit of $2\pi R < \lambda$ (where r is the radius of the particles and λ is the wavelength of the light in the media), only the electric dipole term, developed in Mie's theory, is significant. Then, the cross section can be expressed as the following:

$$C = \frac{(18\pi V \epsilon_2 \epsilon^{3/2})}{\lambda [(\epsilon_1 + 2\epsilon)^2 + \epsilon_2^2]}$$

where ϵ is the dielectric permittivity and taken to be equal to 1.78 and V is the spherical particle volume. It can be expressed as the following:

$$\epsilon = \epsilon_1 + i\epsilon_2$$

The values of ϵ_1 and ϵ_2 are taken from the tabulation by Weaver et al.¹²

If the particle size is comparable with the mean free path of conduction electrons, L_∞ , then the collisions of conduction electrons with the particle surface become important; thus the effective mean free path is less than that in bulk material. The electron energy bands are quantized, and the number of discrete energy levels is of the order of magnitude of the number of atoms in the crystal. The intensities between those levels of the conduction band of metal particle are no longer smeared out thermally if the particles contains only 100 atoms or so. Thereby the intraband transitions of the conduction electrons are influenced, and this leads to a damping of electron motion, which corresponds to the free path effect in the classical method. This damping affects the dielectric constant. A second term ϵ_{20} in the imaginary dielectric permittivity ϵ_2 must be added if the particles are small:

(10) Fragstein, C. V.; Schoenes, F. J. *Z. Phys.* 1967, 198, 477.

(11) Fröhlich, H. *Elektronentheorie der Metalle*; Springer: Berlin, 1936.

(12) Weaver, J. H.; Krafska, C.; Lynch, D. W.; Koch, E. E. *Optical Properties of Metals*; Fachinformationszentrum: Karlsruhe, 1981; Vols. 1 and 2.

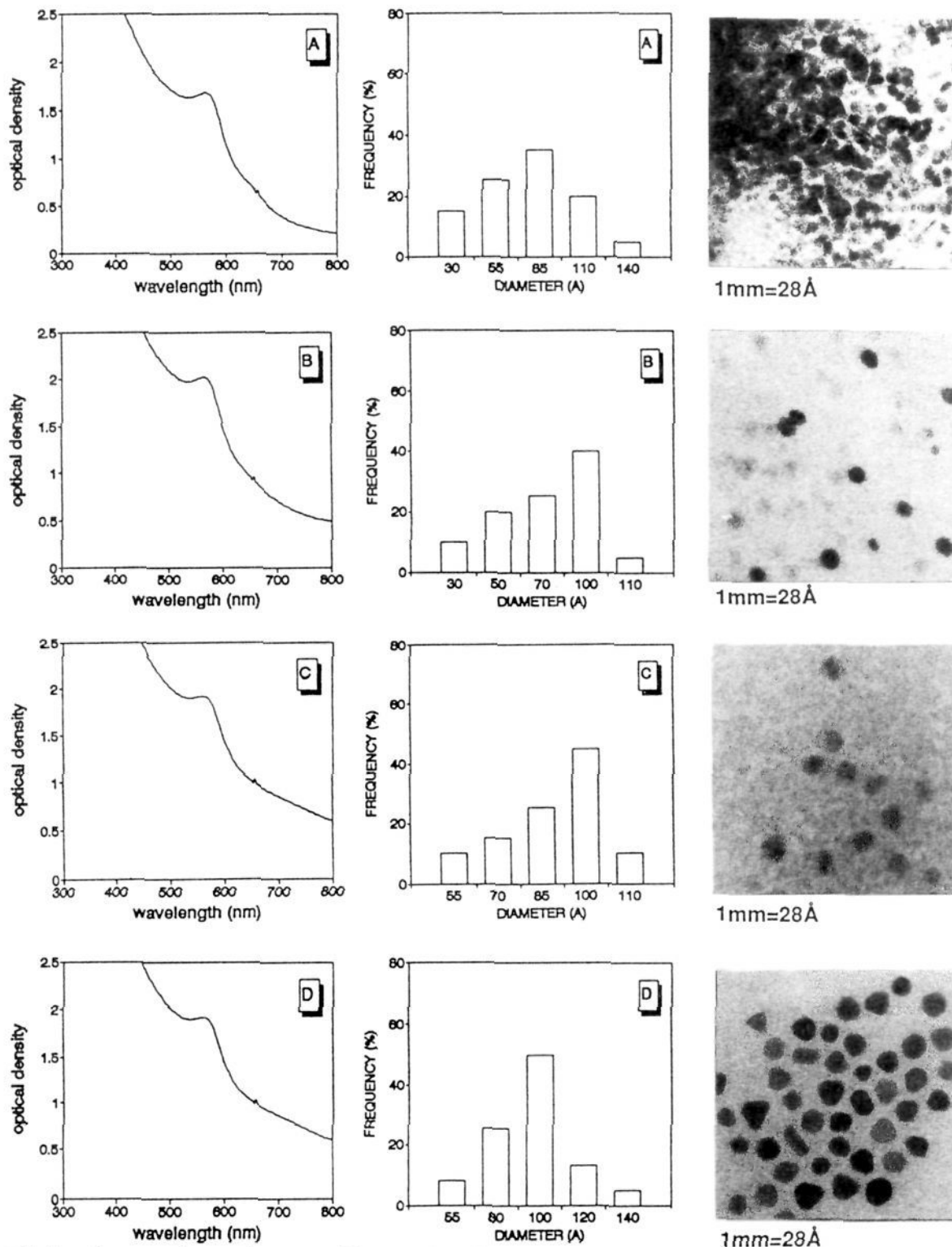


Figure 5. Absorption spectra, electron microscopy, and histograms of metallic copper particles formed in reverse micelles with variable AOT concentrations at $w = 10$: $[\text{Cu}(\text{AOT})_2] = 10^{-2}$ M, $[\text{N}_2\text{H}_4] = 2 \times 10^{-2}$ M. (A) $[\text{AOT}] = 5 \times 10^{-2}$ M (B) $[\text{AOT}] = 2 \times 10^{-1}$ M (C) $[\text{AOT}] = 3 \times 10^{-1}$ M (D) $[\text{AOT}] = 4 \times 10^{-1}$ M. (Reproduced at 85% of original size.)

$$\epsilon_{2Q} = \epsilon_2 + \epsilon_{2s}$$

where ϵ_{2s} is the surface contribution due to the small size of the particle. It can be expressed as:

$$\epsilon_{2s} = L_\infty / r$$

By using this value of ϵ_{2Q} instead of ϵ_2 , the size effect on the optical constant is taken into account. This modified optical

constant is then used in the Mie equations to calculate colloidal absorption bands.

The absorption spectra of the various sizes of small copper particles are simulated for a concentration of copper of 2×10^{-2} M.

For 10-nm-diameter copper particles, the absorption spectrum is characterized by a broad absorption band with a 570-nm peak

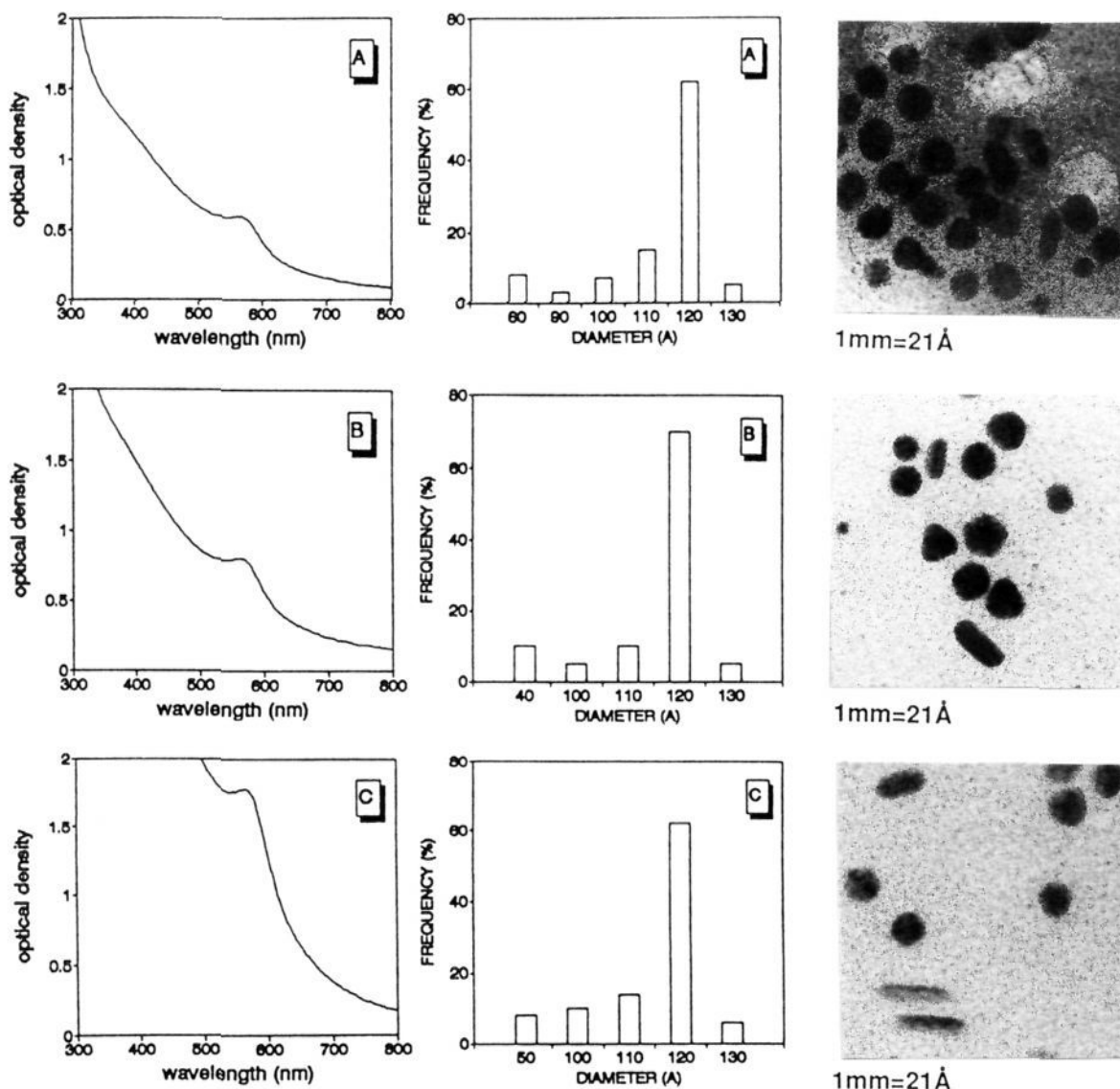


Figure 6. Absorption spectra, electron microscopy, and histograms of metallic copper particles formed in reverse micelles at different copper concentrations: (A) $[\text{Cu}(\text{AOT})_2] = 2 \times 10^{-2} \text{ M}$; (B) $[\text{Cu}(\text{AOT})_2] = 4 \times 10^{-2} \text{ M}$; (C) $[\text{Cu}(\text{AOT})_2] = 10^{-1} \text{ M}$. (Reproduced at 85% of original size.)

attributed to the plasmon band.^{13–15} Yanase and Komiya¹⁶ demonstrated that metallic particles surrounded by an oxide monolayer are characterized by a peak centered at 570 nm, but they also observed a residual absorption at 800 nm due to an oxide monolayer.

From Mie's theory the absorption spectra have been simulated (Figure 1) for particles ranging in size from 1 to 10 nm, and the resulting simulations are compared to the absorption spectrum in the bulk phase. A progressive appearance in the 570-nm plasmon peak occurs upon increasing the size of the copper clusters. It is clear that the copper particles with a diameter below 4 nm are characterized by a strong broadening of the plasmon resonance.

2. Control of the Size of Metallic Particles by the Water Content. Hydrazine, $[\text{N}_2\text{H}_4] = 2 \times 10^{-2} \text{ M}$, as a reducing agent is added to a mixed micellar solution containing copper and sodium AOT ($[\text{AOT}] = 0.1 \text{ M}$; $[\text{Cu}(\text{AOT})_2] = 10^{-2} \text{ M}$). A change in the water content, w of the micelle, is obtained by adding H_2O to the micellar solution before the reaction takes place.

Figure 2 shows the absorption spectra of the colloidal particles, electronic microscopy pictures, and the histograms observed 5 h after the reducing agent was added for reverse micelles with various w values.

At low water content, Figure 2 shows a continuous absorption spectrum with a shoulder at 570 nm. With an increase in the water content, the 570-nm band appears progressively. The electron microscopy pictures show an increase in the size of the particles from 2 to 10 nm upon increasing the water content from 1 to 10. At water contents above 10, the size of the particles remains unchanged but the polydispersity increases. Electron diffractograms, obtained at various water contents compared to a simulated diffractogram of bulk metal copper, are in good agreement. This indicates a crystalline face-centered cubic structure (fcc) with a lattice constant of 3.61.

Similar behavior of the simulated and experimental absorption spectra in Figure 1 and 2 confirms that the plasmon peak can only be observed with relatively large particles (above 3 nm).

3. Size and Polydispersity Control of Metallic Particles. The concentration of copper AOT and hydrazine are kept constant ($[\text{Cu}(\text{AOT})_2] = 10^{-2} \text{ M}$; $[\text{N}_2\text{H}_4] = 2 \times 10^{-2} \text{ M}$). The concentration of sodium AOT increases from 3×10^{-2} to $3.8 \times 10^{-1} \text{ M}$. The increase in AOT concentration corresponds to an

(13) Creighton, J. A.; Eadon, D. G. *J. Chem. Soc., Faraday Trans.* **1991**, 87(24), 3881–3891.

(14) Truong, V. V.; Scott, G. D. *J. Opt. Soc. Am.* **1977**, 67, 502.

(15) Anno, E.; Tanimoto, M.; Yamaguchi, T. *Phys. Rev. B* **1988**, 38, 3521.

(16) Yanase, A.; Komiya, H. *Surf. Sci.* **1991**, 248, 11–19.

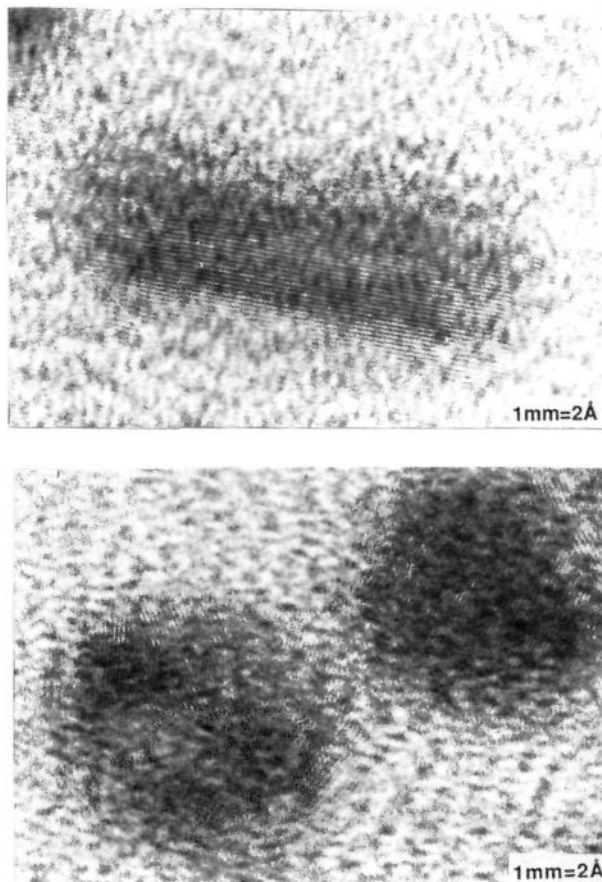


Figure 7. High-resolution electron microscopy of various shapes of copper metallic particles: $[\text{Cu}(\text{AOT})_2] = 4 \times 10^{-2} \text{ M}$, $[\text{N}_2\text{H}_4] = 8 \times 10^{-2} \text{ M}$. Top, cylindrical particles; bottom, spherical particles. (Reproduced at 64% of original size.)

increase in the number of droplets; that is, a decrease of the average number of copper ions per droplet.

(a) Limitation in the Growth of the Particles. At low water content ($w = 1$) and low AOT concentration ($[\text{AOT}] = 3 \times 10^{-2} \text{ M}$ + $[\text{Cu}(\text{AOT})_2] = 10^{-2} \text{ M}$) is observed (Figure 3A) a well-defined peak centered at 570 nm with a low absorption at 800 nm. From the simulated spectrum in Figure 1, this absorption spectrum is characteristic of particles with size greater than 5 nm. Electron microscopy pictures (Figure 3A) show 5-nm-diameter particles with a relatively low polydispersity. With increasing the AOT concentration from 5×10^{-2} to 0.40 M, the absorption spectrum progressively loses the 570-nm peak (Figure 3). This indicates a decrease in the size of the particles, which is confirmed by electron microscopy. The increase in AOT concentration from 5×10^{-2} to 10^{-1} M induces a decrease in the particle size from 5 to 3 nm. At higher AOT concentrations, the resolution of the electron microscope is insufficient to observe particles with sizes below 1 nm. Similar behavior is observed for different micelles with low water contents ($w = 2$ and 3).

At $w = 1$, the absorption spectrum and the electron microscopic imaging are performed 30 min, 5 h, and 24 h after the addition of hydrazine. Figure 4 shows the observed increase in particle size with time. From the histogram, a decrease in the number of 1.4- and 2.1-nm particles and an increase in 2.8-nm clusters are observed (Figure 4). The normalization of the absorption spectra obtained at different times to an arbitrary optical density at 470 nm shows a change in the shape of the absorption spectrum with the appearance of the 570-nm plasmon peak after 24 h. This confirms the electron microscopy data indicating an increase in particle size with time.

Table I. Ratio of the Optical Densities at 800 nm and 570 nm ($\text{OD}_{800}/\text{OD}_{570}$)

w					
6	7	8	9	10	10^a
0.36	0.49	0.43	0.51	0.53	0.17

^a Indicates the result obtained using hydrazine as a reducing agent.

Table II. Radii of Spheres (r_s), Lengths (l_c), and Radii of Cylindrical Clusters (r_c) at Various Copper AOT Concentrations^a

$[\text{Cu}(\text{AOT})_2]$	R_s (nm)	l_c (nm)	R_c (nm)	$[\text{Cu}(\text{AOT})_2]$	R_s (nm)	l_c (nm)	R_c (nm)
10^{-2}	5			4×10^{-2}	6	18	4
2×10^{-2}	6	12	4, 5	10^{-1}	6	22	3

^a Indicates the length and the radii of the copper aggregates obtained before the chemical reaction.

From Figure 4 an increase in the intensity of the absorption spectrum with time can be observed. However, according to the simulated spectra (Figure 1), the change in the size of the particles does not drastically increase the intensity of the absorption spectrum. The increase in the intensity with time can be attributed to an increase in the concentration of the particles.

(b) Limitation in the Polydispersity of the Particle Sizes. At higher water content ($w = 10$) and with increased AOT concentrations, the 570-nm plasmon peak is still present. However, the shape of the absorption spectrum changes with AOT concentration. The average size of the copper cluster remains the same (Figure 5) with an increase in the monodispersity of the particles size. Although the number of copper ions per micelle decreases with increasing AOT concentration, the local concentration remains large. At $[\text{AOT}] = 0.4 \text{ M}$, the copper ion concentration per micelle is equal to 5. Furthermore, compared to $w = 1$, the efficiency of exchange is higher and the interface rigidity is lower. This confirms the role of AOT as a protecting agent, as has been observed with CdS clusters.³

4. Changes in the Shape of the Particles. By using pure copper AOT water-in-oil aggregates; it has been previously shown that a change in the shape of the aggregates is induced by increasing the water content. Droplets are observed at $w = 2$, while cylindrical aggregates are formed at $w = 4$.¹⁷

The reduction of copper reverse micelles was achieved with N_2H_4 as the reducing agent at various surfactant concentrations ($10^{-2} < [\text{Cu}(\text{AOT})_2] < 10^{-1} \text{ M}$; $[\text{N}_2\text{H}_4] = 2 \times [\text{Cu}(\text{AOT})_2]$) with a constant $w \approx 4$.

The shape of the absorption spectrum of the resulting metal clusters is unchanged by increasing the $\text{Cu}(\text{AOT})_2$ concentration. The increase in optical density is due to an increase in the metallic particle concentration with the number of reverse micellar aggregates (Figure 6). At low $\text{Cu}(\text{AOT})_2$ concentration, the clusters are spherical. Upon increasing the $\text{Cu}(\text{AOT})_2$ concentration, formation of cylindrical clusters is observed. The average number of cylindrical clusters remains constant (at about 10%) with 90% of the particles being spherical. However, a further increase in the surfactant concentration induces the formation of longer cylinders with a smaller radii (Table II).

The electron diffraction shows concentric circles characteristic of a face-centered-cubic phase with a lattice dimension equal to 3.61 Å. The distance between the highest density reticular plane (111) can be calculated $(3.61(3))^{1/2} = 2.09 \text{ Å}$. High-resolution electron microscopy of the cylindrical particles (Figure 7, top) shows an interreticular distance of 2 Å. This value is in good agreement with that calculated from the lattice of the bulk phase. Figure 7, bottom shows a high-electronic-resolution image of these spherical particles with various orientations of the reticular planes.

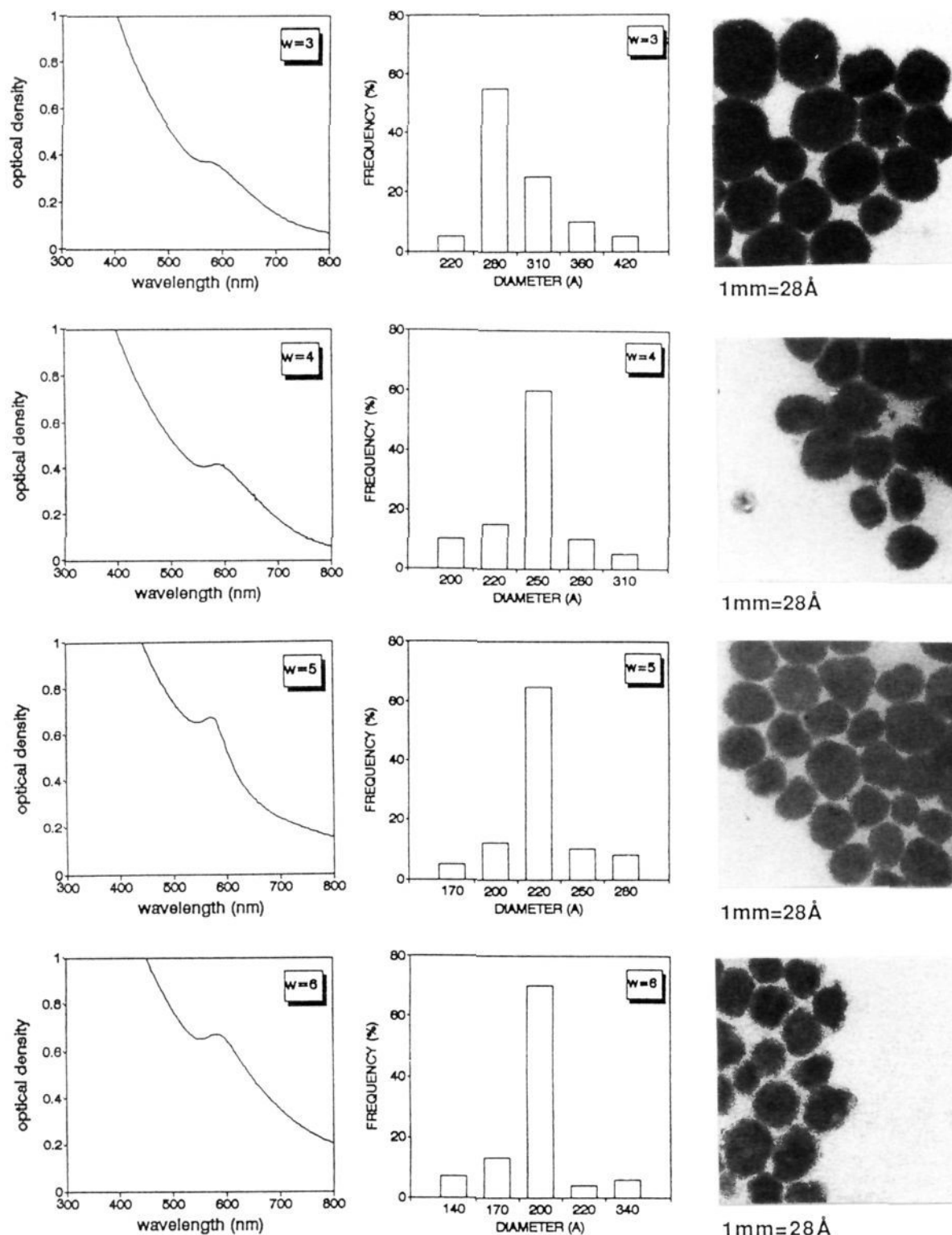


Figure 8. Absorption spectra, electron microscopy, and histograms of metallic copper particles formed in reverse micelles: $[\text{AOT}] = 0.25 \text{ M}$; $[\text{Cu}(\text{AOT})_2] = 10^{-3} \text{ M}$; $[\text{NaBH}_4] = 2 \times 10^{-3} \text{ M}$. (Reproduced at 85% of original size.)

5. Changes of Oxidation State of Clusters. By using sodium borohydride as the reducing agent ($[\text{NaBH}_4] = 2 \times 10^{-3} \text{ M}$; $[\text{AOT}] = 0.25 \text{ M}$; $[\text{Cu}(\text{AOT})_2] = 10^{-3} \text{ M}$) in the absence of oxygen, an absorption spectrum characteristic of metallic particles is observed.

Figures 8 and 9 show a decrease in the size of the particles from 28 to 3 nm upon increasing the water content. At low water content ($w = 3$ and 5), the particles are homogeneously dispersed. Upon increasing the water content from $w = 4$ to 8, the particles

become progressively associated. From electron diffraction patterns for particles formed in micelles with low water content ($3 < w < 5$), the clusters are face-centered cubic with a lattice dimension equal to 3.61, similar to that obtained in metallic bulk phase. At high water content ($w = 9$ and 10), a cubic phase with a lattice parameter equal to 4.27 characteristic of Cu_2O is observed.

The shape of the absorption spectrum of the colloidal particles changes with water content: at $3 < w < 6$, the shapes of the

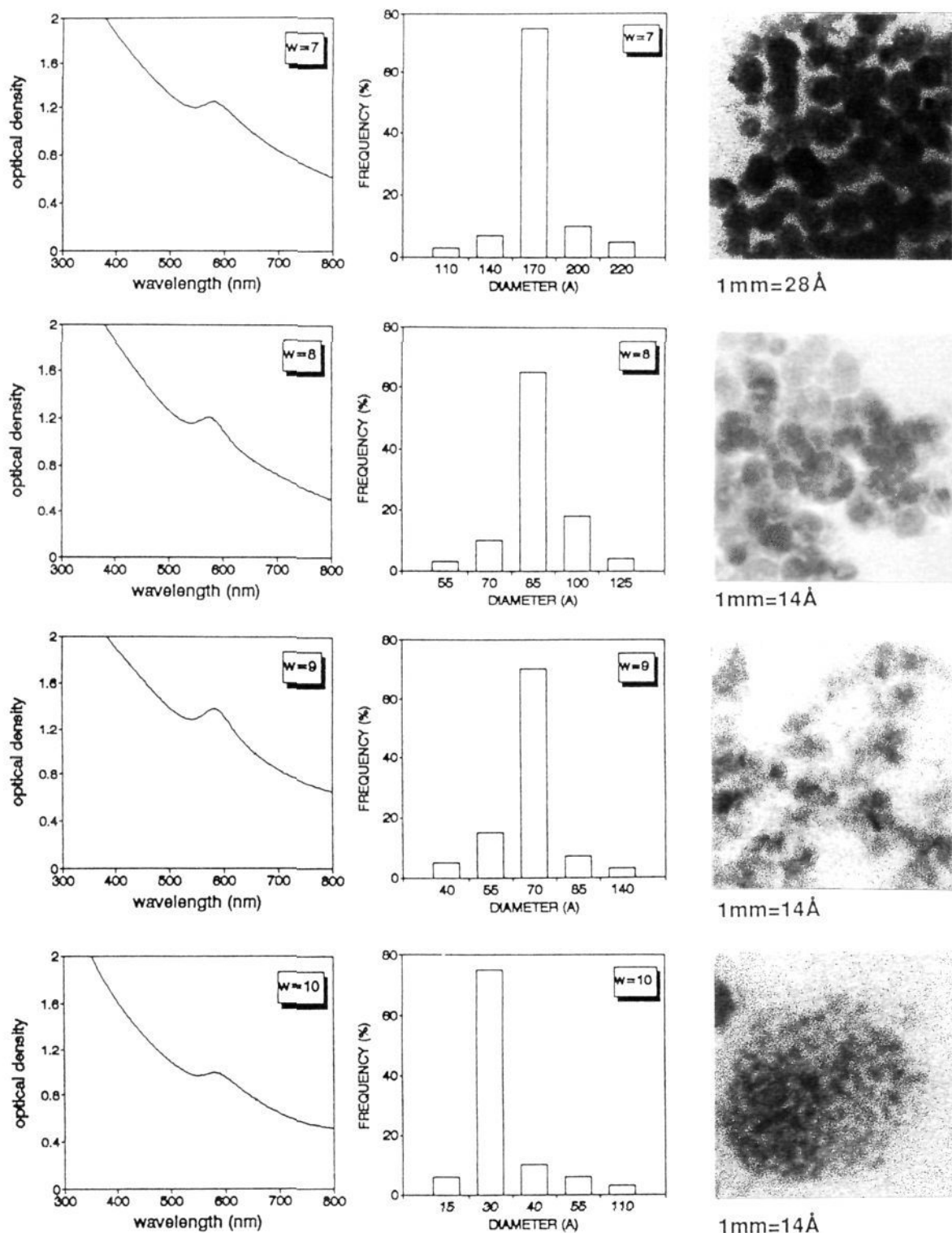


Figure 9. Absorption spectra, electron microscopy, and histograms of metallic copper particles formed in reverse micelles: $[AOT] = 0.25 \text{ M}$; $[Cu(AOT)_2] = 10^{-3} \text{ M}$; $[NaBH_4] = 2 \times 10^{-3} \text{ M}$. (Reproduced at 85% of original size.)

absorption spectra are similar with changes in the intensity and a small residual absorption at 800 nm (Table I). Upon increasing the water content, an absorption around 800 nm appears (Table I). According to Yanase and Komiyama¹⁶ the 800-nm absorption is attributed to an oxide monolayer surrounding the metallic cluster.

By comparing the microscopy data and the absorption spectra, it can be deduced that at low water content, metallic particles are formed. By increasing the water content, the metallic particles

are surrounded by mono- and multilayers of oxide, which prevents further growth of the particles. At higher water content (above $w = 8$), pure copper oxide particles are obtained. This is confirmed by the fact that below $w = 7$ electron microscopy images show well-dispersed particles, whereas at $w = 7$ and 8 they are associated. This is probably due to the high affinity of the surfactant for the oxide. At $w = 9$ and 10, the electron microscopy images do not show the presence of metallic particles. These data could be related again to the water structure in the water pool (Table III).

Table III. Variation of the Size of the Clusters with Water Content and Reducing Agent after 5 h

reducing agent	w	particle diameter (Å)	oxidation state
hydrazine	1-20	28-100	metallic particles
sodium borohydride	3-10	280-30	metallic particles → oxide particles

Conclusion

Reverse micelles are able to limit the size of growing copper metallic particles from 2 to 10 nm. The growth of the particles

can be prevented by the local structure of the reverse micelle at low water content (Table III), by the number of copper ions formed, and by the kinetics of the micellar exchange between droplets. The shape of the metallic clusters is changed with the shape of the microaggregates containing the reactants. By increasing the water content and using NaBH_4 as a reducing agent, (Table III), the microenvironment of the clusters can be changed either to accommodate an oxide monolayer surrounding the metallic particles or, with the formation of borohydride, a copper oxide cluster. Formation of metallic particles is observed in the presence and in the absence of oxygen, by using hydrazine or sodium borohydride, respectively.